NASA TECHNICAL NOTE

NASA TN D-5013

rpt. 1, c.1

NASA TN D-5013

A 1-MEGAWATT REACTOR DESIGN FOR BRAYTON-CYCLE SPACE POWER APPLICATION

I - Thermal Analysis and Core Design

by Charles L. Whitmarsh, Jr., and Paul T. Kerwin

Lewis Research Center
Cleveland, Ohio

NATIONAL AERONAUTICS AND SPACE ADMINISTRATION • WASHINGTON, D. C. • FEBRUARY 1969

NASA TN D-5013

A 1-MEGAWATT REACTOR DESIGN FOR BRAYTON-CYCLE SPACE POWER APPLICATION

I - THERMAL ANALYSIS AND CORE DESIGN

By Charles L. Whitmarsh, Jr., and Paul T. Kerwin

Lewis Research Center
Cleveland, Ohio

NATIONAL AERONAUTICS AND SPACE ADMINISTRATION

For sale by the Clearinghouse for Federal Scientific and Technical Information
Springfield, Virginia 22151 – CFSTI price $3.00

ABSTRACT

Thermal-hydraulic calculations were performed for a 1-MW gas-cooled reactor designed to retain all fission gases and to operate for 25 000 hours with a coolant outlet temperature of 1650 K. These data were combined with neutronics data from part II in an effort to minimize core size. Parameters investigated were fuel-element configuration, fuel-cladding temperature, radial and axial power distributions, coolant inlet temperature, coolant pressure, and reactor pressure drop.

A 1-MEGAWATT REACTOR DESIGN FOR BRAYTON-CYCLE SPACE POWER APPLICATION

I - THERMAL ANALYSIS AND CORE DESIGN

by Charles L. Whitmarsh, Jr., and Paul T. Kerwin

Lewis Research Center

SUMMARY

Parametric studies were performed relating core size to such design variables as temperature, temperature rise, pressure, pressure drop, and power distribution. Acceptable core configurations were determined subject to the restraints of heat transfer, critical fuel mass, and sufficient fuel cladding to retain fission gases. A reactor core diameter of 31.7 centimeters was then selected from the parametric studies as the minimum value consistent with the engineering limitations imposed on the design procedure.

The selected core design was a right circular cylinder composed of tungsten - 25-weight-percent-rhenium fuel pins loaded with enriched uranium dioxide. The core was surrounded radially by a 0.95-centimeter-thick tungsten - 25-weight-percent-rhenium pressure vessel and a 7.62-centimeter-thick beryllium oxide reflector, and axially by 1.27-centimeter-thick tungsten end plates. Control was achieved by axial movement of radial reflectors. Fuel enrichment was varied radially to flatten the radial power to a peak-to-average ratio of 1.05. A space was provided for fission gases at the end of each fuel pin. With a coolant gas temperature of 1650 K, the calculated maximum fuel-cladding temperature during normal operation was 1805 K.

Parametric calculations indicated core size to be sensitive to fuel-cladding thickness. As core temperatures were increased the resulting increased fuel-cladding thickness dominated the opposing effect of better heat transfer, and thus caused the required core size to increase. Core size was insensitive to a ±60 K variation in the coolant gas inlet temperature. The effects on core size of varying coolant gas pressure, core pressure drop, space for fission gas, and axial power shape were determined by the particular design conditions and could not be generalized.

INTRODUCTION

Nuclear-reactor-powered Brayton-cycle systems are of interest for space applications requiring electric power in the range of tens of kilowatts to megawatts (refs. 1 and 2). The Brayton system has the advantages of a noncorrosive working fluid, a compact power source, high cycle efficiency, and a relatively well-developed component technology; but it also has such disadvantages as large piping and components to be shielded and large radiator area. The potential applications of this reactor system are generally limited at high powers by radiator area and weight.

While both liquid-metal-cooled and gas-cooled reactors can serve as heat sources for Brayton systems, only gas-cooled reactors are considered herein. Design goals of high-temperature operation and small core size have led to typical reactor core characteristics of highly enriched, highly dense fuel systems, refractory-metal structural components, and external control systems based on either leakage and/or absorption of neutrons (ref. 3).

This report is a study of gas-cooled reactors designed for use in an "advanced-state-of-the-art" Brayton-cycle space power system. The objective is a preliminary reactor design that would produce 1 megawatt of thermal power for 25 000 hours with a turbine inlet temperature of 1650 K and that would retain all fission gases in the core. A single-loop system was selected so that the reactor coolant outlet temperature could be assumed to be equal to the turbine inlet temperature. The reactor core is composed of either fuel-pin bundles or a solid matrix fuel penetrated by coolant passages. Since reactor size, with its associated shield weight penalties, is of major importance to space power systems, design effort is concentrated on minimization of core size.

The design study is presented in two parts: I - THERMAL ANALYSIS AND CORE DESIGN, and II - NEUTRONICS DESIGN, each part being issued as a separate report. Part I combines neutronics information from part II with heat-transfer and fluid flow calculations to define the internal core configuration and to show the effect of various design parameters on core size. It also includes the Brayton system analysis necessary to establish reactor design parameters. Part II presents the nuclear calculations and defines the control system and materials of construction.

More specifically, this report, part I - THERMAL ANALYSIS AND CORE DESIGN, presents parametric results showing the effects on core size of specific design variables (e.g., maximum fuel-cladding temperature, axial and radial power profiles, fuel material, containment volume for fission gases, pressure drop, coolant inlet temperature, and coolant pressure). Data from these calculations were used to select the design conditions for the minimum-size core consistent with the design criteria. Based on this set of conditions, a reactor core configuration was calculated which was considered to be the recommended design.

REACTOR CONCEPT

A cycle analysis (appendix A) provided the recommended Brayton-cycle conditions shown in figure 1. This analysis defined the reactor inlet and outlet pressures (1.74 and 1.68 MN/m^2 or 252 and 244 psia) and inlet temperature (1190 K). Turbomachinery considerations indicated that the coolant should be a mixture of helium and 60-volume-percent xenon (He-60Xe) flowing at the rate of 8.5 kilograms per second. The reactor configuration presented in figure 2 is a result of the neutronics analysis (ref. 4). This information, combined with the given conditions of a 1-megawatt gas-cooled reactor operating for 25 000 hours with an outlet temperature of 1650 K, led to the following reactor concepts.

The reactor core is a cylinder with a diameter of about 30 or 40 centimeters and a length-to-diameter ratio of 1, which was selected to minimize the weight of possible 4π shield designs. The core configuration was limited to either (1) bundles of fueled tubes with the coolant gas flowing external to and parallel to the tubes (pin core) or (2) a number of hexagonal fuel elements fitted together and penetrated by coolant passages (matrix core). In the pin cores, space for fission gases is provided at the end of the fuel tubes. No such space is provided in matrix cores because fission gases are assumed to be retained within the fuel material. The core is contained in a 0.95-centimeter-thick tungsten - 25-weight-percent-rhenium pressure vessel (appendix B) and has 1.27-centimeter-thick tungsten end plates at both ends. Two fuel arrangements in the core are considered: uniform distribution of fully enriched fuel (93.2-percent U^{235}), and nonuniform distribution in which fuel enrichment is varied in six radial core zones to achieve a flattened power distribution (ref. 5). The fuel for pin cores is uranium dioxide

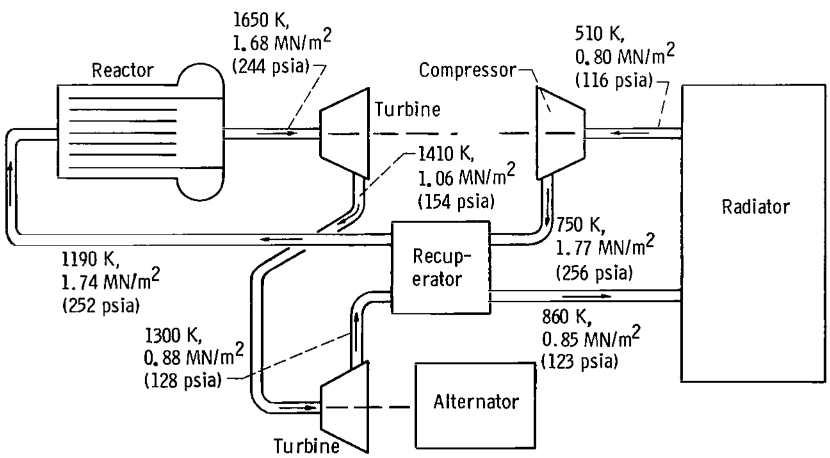

Figure 1. - Schematic of Brayton-cycle system. Working fluid, He - 60-volume-percent Xe gas mixture (molecular weight, 80 kg/kg-mole); mass flow rate, 8.5 kilograms per second.

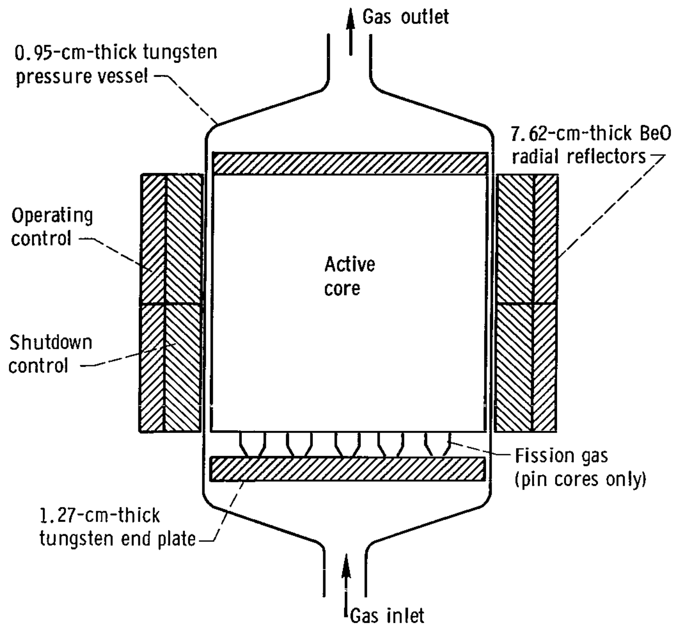

Figure 2. - Schematic of gas-cooled reflector-controlled fast-spectrum reactor.

(UO_2) enriched with uranium-235 (U^{235}) and for matrix cores is enriched U^{235} in a 60-volume-percent UO_2 - tungsten cermet. Fuel cladding is tungsten - 25-weight-percent rhenium (W-25Re).

Reactor control is achieved by axial movement of beryllium oxide (BeO) radial reflectors. The total reflector thickness of 7.62 centimeters provides a control range of greater than 10 percent reactivity, the specific value being dependent on core size and fuel distribution. The reflector is divided radially into two segments; the outer segment is used for operating control and the inner segment for shutdown control. No coolant passages through the reflector were provided because forced cooling was considered unnecessary (appendix C).

ENGINEERING CONSIDERATIONS

Because of the great number of variables present in any reactor design procedure, many constraints must be set beforehand to facilitate parametric analyses. Some might properly be called design constraints, which are in the nature of fabrication and/or material limits and are based primarily on engineering judgement. Other related constraints could be considered as "ground rules" (i.e., conditions and/or procedures established prior to, and used throughout, the study). A list of both types of constraints follows:

(1) Fuel-to-cladding gap at operating temperature equals 0.005 centimeter in pin-type cores. Determination of gap effects was considered beyond the scope of this study, and therefore the same value was selected for all designs.

(2) The creep limit is 1 percent in 25 000 hours in the fuel cladding of pin-type cores. The detailed mechanical design required to determine allowable creep limits was beyond the scope of this study.

(3) The fuel diameter must be ≥0.5 centimeter in pin-type cores. This diameter was estimated to be a lower limit for fuel-element fabrication.

(4) The fuel-cladding thickness must be ≥0.025 centimeter in pin-type cores. This was estimated to be a lower limit of wall thickness for fabrication of refractory-metal tubes.

(5) No fuel melting is permitted in pin cores. Thus, in a UO_2 fuel pin the maximum allowable temperature is 2750 K during normal operation. The problems associated with molten fuel were not considered.

(6) The maximum allowable fuel temperature for matrix core designs is 1900 K. This was estimated to be the maximum temperature at which the fuel could operate for 25 000 hours and still retain all fission gases.

(7) In pin-type cores, total release of fission gases from the fuel must occur when the average fuel centerline temperature in the hot channel exceeds 2025 K, and 50 percent must be released at lower temperatures. A conservative value was selected from a compilation of data on fission gas release from UO_2 in reference 6, which included the most extreme datum point. Calculations were simplified by assuming only two levels of release, 50 and 100 percent.

(8) Axial power shapes can be described by the function $\cos \pi Z/L_e$, where Z is the axial position variable with a $L/2$ to $-L/2$ range, L is the core length, and L_e is the extrapolated core length. In a fast-spectrum core with thin reflectors, flux shapes approximate the cosine shape derived from bare-core reactor theory. Only symmetric shapes with equal reflector thicknesses at each end of the core were considered.

(9) In zoned cores, the radial power shape is assumed to be flat and at its maximum value in each zone. This assumption was made to simplify the calculational procedure.

(10) An overall hot-channel factor of 1.1 is assumed. Lack of a detailed mechanical design prevented the calculation of a hot-channel factor. The relatively low value of 1.1 was selected on the basis that good quality control would be used in the production of reactors for space.

(11) Pin-type cores can be constructed such that pin bundles are sufficiently rigid radially to prevent bowing. This problem was assumed to be solvable in detailed mechanical design and not within the scope of this study.

TABLE I. - DESIGN MODEL PARAMETER VALUES

FOR PIN CORE CALCULATIONS

Parameter	Comment
Reactor power, 1MW Core life, 25 000 hr Coolant outlet temperature, 1650 K Fuel-cladding hot gap, 0.005 cm Hot-channel factor, 1.1 Core length-to-diameter ratio, 1.0	Fixed values for all designs
Axial power factor, 1.27	Based on a 1.27-centimeter tungsten end plate at either end of the core (ref. 4)
Radial peak-to-average power ratio, 1.05	Estimated value obtainable by radial fuel distribution (ref. 5)
Actual pin length to fuel length ratio, 1.1	Allowance of 10 percent of core volume for fission gas chamber
Coolant inlet temperature, 1190 K Average core pressure, 1.71 MN/m^2 (248 psia) Reactor pressure drop, 55 kN/m^2 (8 psia, or 3 percent $\Delta p/p$) Fuel, $U^{235}O_2$	Recommended conditions from Brayton-cycle study (appendix A)

(12) The space allotted to fission gases was assumed to be equal to 10 percent of the volume of a fuel pin. Since the space was arranged at the end of a fuel pin, the resultant pin length is 1.1 times the length of the fuel.

(13) Of the total pressure drop through the core, 25 percent was allocated to inlet and outlet losses. This value was calculated for a typical core configuration and then considered to be constant for all configurations (appendix D).

(14) Fuel-cladding thickness for fuel pins was determined solely by fission gas pressure. Mechanical and thermal stresses in the tube wall were considered to be insignificant compared with the tangential stress resulting from the internal gas pressure.

(15) For all matrix core designs the thickness of coolant hole liners (cladding) was 0.025 centimeter, an additional 15 percent of the coolant liner material was added to account for the cladding around the hexagonal fuel elements, and a core volume fraction of 5 percent was allowed for intracore expansion. These factors were based on previous designs.

(16) Incompressible flow equations were utilized to describe the gas coolant. These equations were considered to be sufficiently accurate because of the low Mach numbers

TABLE II. - DESIGN MODEL PARAMETER VALUES

FOR MATRIX CORE CALCULATIONS

Parameter	Comment
Reactor power, 1 MW	Fixed values for all designs
Core life, 25 000 hr	
Coolant outlet temperature, 1650 K	
Coolant hole cladding, 0.025 cm	
Hot-channel factor, 1.1	
Core length-to-diameter ratio, 1.0	
Axial power factor, 1.27	Based on a 1.27-centimeter tungsten end plate at either end of the core (ref. 4)
Radial peak-to-average power ratio, 1.05	Estimated value obtainable by radial fuel distribution (ref. 5)
Coolant inlet temperature, 1190 K	Recommended conditions from Brayton-cycle study (appendix A)
Average core pressure, 1.71 MN/m^2 (248 psia)	
Reactor pressure drop, 55 kN/m^2 (8 psia or 3 percent $\Delta p/p$)	
Fuel, 60 vol. % $U^{235}O_2$-W	

(~0.1) existing at design conditions (appendix E).

The design conditions are summarized in table I for pin cores and in table II for matrix cores.

CALCULATIONAL PROCEDURE

In high-temperature compact reactors the fractional core volume occupied by fuel cladding is of the order of 10 to 30 percent, and therefore has a significant influence on core size. Because of this influence, the fuel-cladding thickness in pin core designs was treated as a variable which was dependent on operating conditions, as opposed to constant cladding thickness determined by some property such as material fabricability. The calculational procedure developed was (1) to select a core diameter, (2) to calculate the number and outside diameter of the pins based on the required heat transfer and pressure drop, and (3) to determine the tube wall thickness required to retain the pressure from the fission gases produced during operation. The resulting configuration was then compared with criticality data to determine whether it contained sufficient fuel to operate neutronically. The procedure for matrix cores was similar except that fuel-cladding (coolant passage liner) thickness was set for all core designs at 0.025 centimeter on the basis of fabricability.

The specific procedure used for pin core design is summarized as follows:

(1) Values for coolant conditions were selected primarily on the basis of cycle conditions (e.g., mass flow rate, inlet temperature, outlet temperature, inlet pressure, and reactor pressure drop). The core properties (ratio of pin length to fueled length, axial power shape factor, maximum fuel-cladding temperature in an average channel, and core diameter) were selected. Then the resulting Reynolds number, coolant flow volume fraction, and outside diameter of the fuel pins were calculated. These results were based on a cylindrical core with a length-to-diameter ratio of 1, with all material properties evaluated at core average temperatures and with fuel pins arranged on a triangular lattice. Relatively standard methods were used in the calculations, including the Dittus-Boelter heat-transfer correlation and the incompressible flow equations (ref. 7). The Dittus-Boelter correlation was modified, on the basis of experimental data for subsonic high-temperature airflow through tubes (ref. 8), to account for the large difference between bulk fluid and tube surface temperatures.

(2) Values for the hot-channel factor and the peak-to-average radial power ratio were selected. The allowable end-of-life stress for 1 percent creep during core life (25 000 hr) was determined on the basis of hot-channel temperatures and a linearly increasing stress during the core life (appendix F).

(3) The percentage of the fuel which would be fissioned after 25 000 megawatt-hour operation %B was estimated, and the pressure from the resulting fission gas buildup was calculated at hot-channel conditions (appendix G). The tube wall thickness required to limit the creep caused by this pressure to 1 percent over the core life was then determined. The volume of fuel (inside the pins) was calculated, and, since the required number of fissions was known for 25 000-megawatt-hour burnup, the actual %B could be calculated. Step 3 was iterated until the estimated %B equalled the actual %B.

(4) This particular configuration was then characterized by relating the core diameter to the fuel volume fraction f_F (i.e., the space available for fuel after the flow, cladding, and void requirements were met).

This procedure was repeated for different core diameters, and the resulting data were used to plot a curve of core diameter as a function of fuel concentration, any point on which represented a configuration that met the heat-transfer, pressure drop, and stress requirements for a particular set of conditions. This curve was then superimposed onto a criticality curve relating core diameter to required fuel concentration for a reactor with sufficient reactivity to operate at 1 megawatt for 25 000 hours (ref. 4). Only points where f_F equaled or exceeded the required fuel volume fraction for criticality represented a permissible design configuration. Minimum core size occurred where f_F equaled the critical fuel volume fraction.

PARAMETRIC RESULTS

The effect of several design parameters on core size was investigated both to determine recommended conditions for a reference design and to indicate the trend to be expected should other designs be formulated. Most parametric changes in pin core designs affected both heat transfer and fuel-cladding thickness, which, in general, have opposing influences on core size. For example, parametric changes which increased the heat transfer per unit area also necessitated increased fuel-cladding thickness. The fuel volume fraction was increased by the greater heat transfer per unit area, thereby reducing required core size, whereas fuel volume fraction was reduced by the increased fuel-cladding thickness, thereby increasing required core size. Thus, although the trends of the independent effects were reasonably well known, the net effect was not so obvious. Matrix core designs, because of the assumption that the fuel matrix will contain all fission gases, are not subject to changes in cladding thickness but are affected only by those parameters that influence heat transfer per unit area.

Fuel-Cladding Temperatures

The effect of varying the fuel-cladding temperature in pin core designs was determined on a core model with the parameters in table I. As expected, increasing the temperature increased heat transfer per unit area (lowered required heat-transfer area for a given core size), thereby allowing pin size to increase. This increase, in turn, meant that fuel volume fraction increased. However, increasing the temperature also decreased the allowable material stress limit for the fuel cladding and increased the fission gas

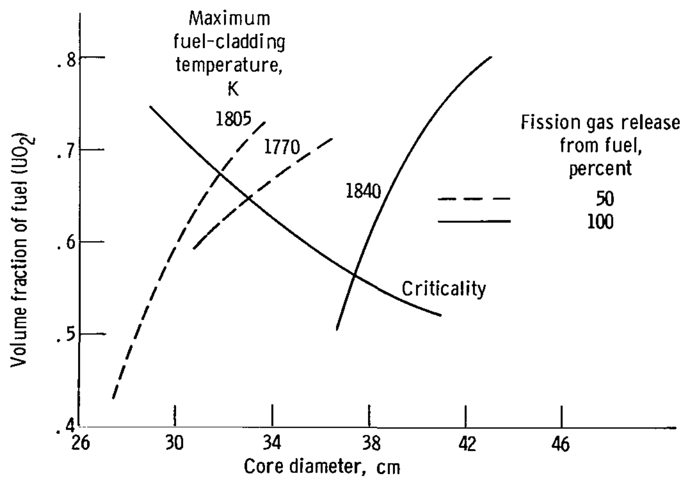

Figure 3. - Effect of fuel-cladding temperature on required core size of pin core designs.

pressure; both effects caused the required fuel-cladding thickness to increase, thereby reducing fuel volume fraction.

The net effect of these phenomena on core size is shown in figure 3, which indicates that an optimum value (minimum core size) for maximum fuel-cladding temperature occurs near 1805 K. However, this optimum is the result of certain design criteria, as well as the physical processes discussed in the preceding paragraph. As the temperature was reduced below 1805 K, calculated fuel-cladding thicknesses became less than the 0.025-centimeter lower limit criterion. Therefore, for these designs the cladding thickness was set at 0.025 centimeter. This additional cladding reduced the available space for fuel, thereby requiring that the core size be increased to maintain sufficient fuel for criticality. As the temperature was increased above 1805 K, fuel temperatures were increased from the region of 50-percent fission gas release to 100 percent (fission gas release criterion). The additional pressure inside the fuel pins required increased fuel-cladding thicknesses and increased core size.

In an effort to separate the physical processes from the effects of the design criteria, the temperature effect was isolated by performing additional calculations in which 100-percent fission gas release was assumed in every case. The results in figure 4 show that core size increased with increasing fuel-cladding temperature, thereby indicating that the effect of increased fuel-cladding thickness predominated over increased heat transfer per unit area.

The temperature range for this parametric study was restricted by the design conditions. At maximum fuel-cladding temperatures, less than 1770 K, the pin diameter became less than the 0.5-centimeter fabrication lower limit for core sizes near the

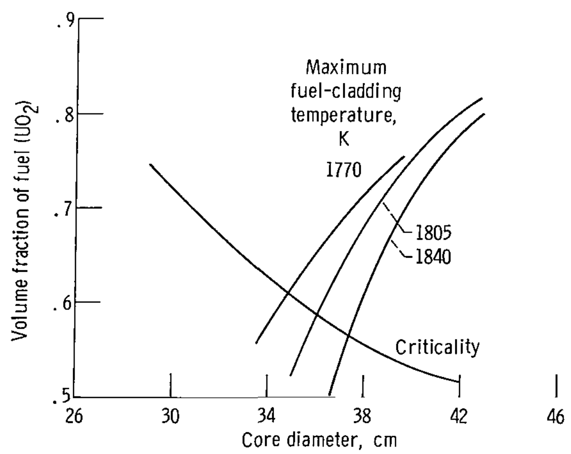

Figure 4. - Effect of fuel-cladding temperature on required core size of pin core designs with total release of fission gas from fuel.

critical diameter; and at temperatures greater than 1840 K the maximum fuel centerline temperature exceeded the melting point of UO_2.

In matrix core designs the temperature of the coolant passage liners corresponded to the fuel-cladding temperature of pin cores. Because the liners and the fuel matrix were assumed to be in intimate contact in these designs, the liner temperature was used instead of the fuel temperature as the criterion for fission gas retention. Although 1890 K was considered to be the maximum allowable temperature, designs at 2000 K were calculated to indicate the potential size reduction with advanced material technology. Design parameters for the calculational model are listed in table II.

Figure 5 indicates that the core diameter can be reduced 1.6 centimeters for a 110 K rise in fuel surface (cladding) temperature. Also, the increase in fuel volume fraction with increasing core size was about 0.5 percent per centimeter of diameter. Both of these effects were smaller than for pin cores because only the heat-transfer conditions were influenced by the parametric changes and there was no counteracting effect of a change in cladding thickness.

The minimum matrix core diameter was larger (about 37 percent) than the minimum pin core diameter primarily because of lower uranium density in the cermet fuel material. The volume available for fuel was actually higher in the matrix cores, but only 60 percent of the volume was UO_2. If 80-volume-percent UO_2-W were used, the critical core diameter would be reduced to about 34 centimeters.

Radial Power Distribution

To determine the overall effect of radial power flattening on core design, the neu-

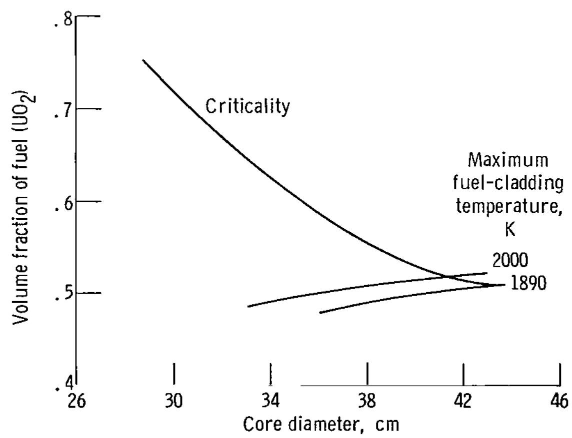

Figure 5. - Effect of fuel-cladding temperature on required core size of matrix cores.

tronic effects from reference 4 were combined with the thermodynamic effects calculated herein. The data in figure 6 indicate a 9-percent reduction in core diameter when the unzoned core (with a peak-to-average power ratio of 1.35) was radially power flattened to a peak-to-average ratio of 1.10. Additional flattening to a peak-to-average ratio of 1.05 resulted in another 1-percent reduction in core diameter. (Note that in fig. 6 the core diameters are defined by the intersections of curves with the same power ratios.) This additional power flattening also reduced the average fuel centerline temperature in an average channel from 2025 to 1990 K (table III).

Comparison was made on the basis of the best maximum fuel-cladding temperature for each level of radial power flattening. Thus, for radial power ratios of 1.05 and 1.10 the maximum fuel-cladding temperature was 1805 K, and for 1.35 it was 1920 K. These temperatures were determined by an analysis similar to that of figure 3.

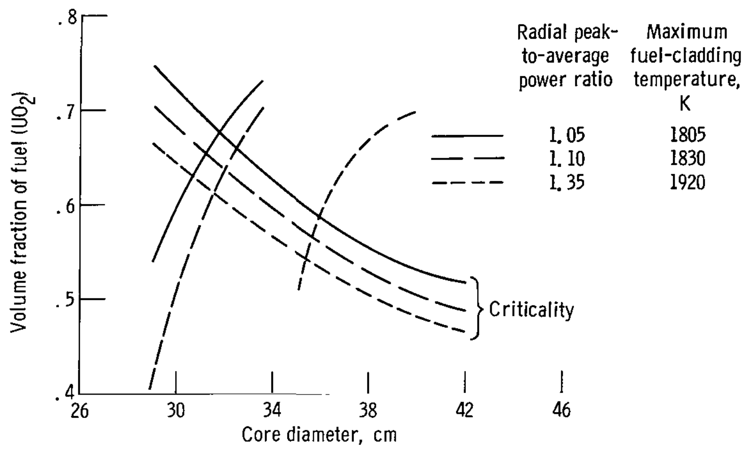

Figure 6. - Effect of radial power flattening on core size of pin core designs.

TABLE III. - EFFECT OF RADIAL PEAK-TO-AVERAGE POWER RATIO ON CORE TEMPERATURES IN PIN CORE DESIGNS

Radial peak-to-average power ratio	Maximum fuel-cladding temperature in average channel, K	Maximum fuel-cladding temperature in hot channel, K	Average[a] fuel centerline temperature in hot channel, K
1.05	1720	1805	1990
1.10	1720	1830	2025
1.35	1680	1920	1825

[a]At core size required for criticality (fig. 6).

Matrix core calculations at a peak fuel-cladding temperature of 1890 K indicated essentially no difference in critical core size for the 1.05 and 1.10 cases. The use of 1.35 for the peak-to-average power ratio made heat removal impossible with the given coolant inlet and outlet temperatures.

Fission Gas Chamber

Since fuel-cladding thickness appeared to be a significant factor in determining the size of pin cores, the effect of enlarging the volume for fission gas containment (to reduce the pressure buildup in fuel pins) was investigated. However, an opposing effect (increased core size) resulted because the ratio of pin length to active core length was increased from 1.1 to 1.2. This lengthened the flow path through the core which, for a constant pressure drop and core diameter, required that the free-flow area be increased, pin diameter be reduced, and the number of pins be increased.

Calculations were performed using the maximum fuel-cladding temperature for minimum size (1805 K from fig. 3). The data presented in figure 7 indicate a reduction of only 1 percent in critical diameter. However, at these parametric conditions, the effect on core size was obscured by the minimum fabrication limitation on fuel cladding of 0.025 centimeter. In order to illustrate the full effect of doubling the size of the fission gas chamber, calculations were made using the criterion of 100-percent fission gas release for all cases. The results plotted in figure 7 indicated a 9-percent reduction in critical core diameter.

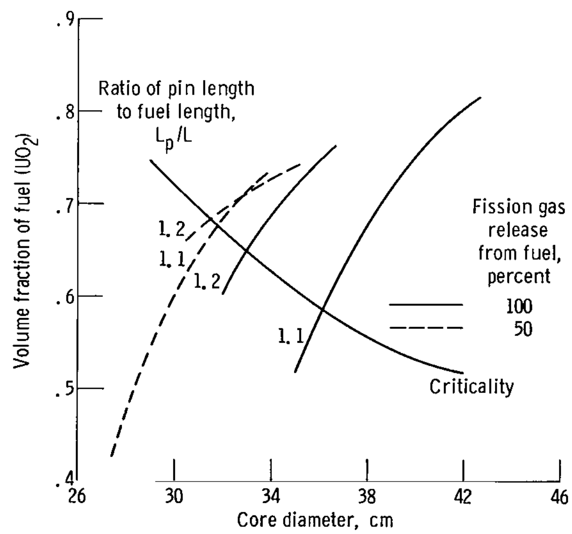

Figure 7. - Effect of fission gas containment chamber on size of pin core designs. Maximum fuel-cladding temperature, 1805 K; radial peak-to-average power ratio, 1.05.

Axial Power Distribution

The axial power distribution was determined by the reflectivity of components located at either end of the reactor core. The neutronics analysis established that the assumed 1.27-centimeter-thick tungsten end plates located at either end of the core provided sufficient reactivity for the reactor system. In lieu of a detailed stress design this configuration was considered adequate for the mechanical design and was used for the thermodynamic analysis. The resulting axial shape factor (obtained by fitting the calculated axial power distribution) was $\cos \pi Z/L_e$, where Z ranged from $-L/2$ to $L/2$ and L_e/L was 1.27. Also, the peak-to-average power ratio was calculated to be 1.31.

In the event that the use of a larger tungsten end plate (or axial reflector) might be required for structural support, calculations were performed for an L_e/L of 1.5. The results obtained on a core model with the reference design parameters from table I indicated that less than a 1-percent change occurred in the relation of fuel volume fraction to core size. However, the core configuration and flow conditions were affected. Data generated for a 29-centimeter-diameter core indicated that when L_e/L was increased, free-flow volume increased while the Reynolds number, fuel-pin diameter, and fuel temperature all decreased (table IV). Similar effects of the same magnitude were observed in calculations on matrix cores.

Coolant Inlet Temperature

The selection of reactor coolant inlet temperature was based on the cycle analysis performed in appendix A. However, the cycle calculations were not sensitive to the

TABLE IV. - EFFECT OF AXIAL SHAPE FACTOR ON SELECTED PARAMETERS OF PIN CORE DESIGNS

[Core diameter, 29 cm; maximum fuel-cladding temperature, 1805 K.]

Axial shape factor, L_e/L	Fuel volume fraction	Reynolds number	Free-flow volume fraction	Fuel-pin diameter, cm	Average fuel centerline temperature in hot channel, K
1.27	0.540	1.65×10^4	0.223	0.823	1970
1.50	.535	1.39	.240	.681	1875

specific value selected. Therefore, thermodynamic calculations were performed with the coolant inlet temperature varied ±60 K to determine whether any potential existed in the reactor design for core size reduction.

Data calculated for a 30.5-centimeter core with a maximum fuel-cladding temperature of 1805 K and reference core parametric values (table I) indicated that a 120 K rise in coolant inlet temperature caused a decrease of allowable fuel volume of 8 percent. Extrapolation of these data resulted in a 2-percent increase in the critical core diameter, thereby indicating the relative insensitivity of core size to coolant inlet temperature (see table V).

Other effects of increasing coolant inlet temperature were increased free-flow volume and decreased fuel-pin diameter and fuel temperature.

Coolant Pressure

The average coolant pressure was also selected on the basis of cycle analysis. To determine whether a potential existed in the reactor design for core size reduction, calculations were made on cores using the reference-design parameter values (table I) with a coolant pressure of 2.76 meganewtons per square meter (400 psi). Data for a 35.1-centimeter-diameter core with a maximum fuel-cladding temperature of 1805 K indicated

TABLE V. - EFFECT OF PERTURBATIONS IN COOLANT INLET TEMPERATURE ON CHARACTERISTICS OF PIN CORE DESIGNS

[Core diameter, 30.5 cm; maximum fuel-cladding temperature, 1805 K.]

Coolant inlet temperature, K	Coolant temperature change across reactor, K	Fuel volume fraction	Reynolds number	Free-flow volume fraction	Pin diameter, cm	Average fuel centerline temperature in hot channel, K	Critical core diameter,[a] cm
1130	516	0.647	1.72×10^{4}	0.173	1.12	1990	31.4
[b]1190	460	.619	1.71	.201	.978	1980	31.7
1250	404	.593	1.65	.230	.808	1910	32.1

[a]Obtained by extrapolating fuel volume fraction against core diameter to an intersection with a criticality curve.

[b]Reference value from cycle study.

TABLE VI. - COOLANT PRESSURE VARIATION EFFECT ON

PARAMETERS OF PIN CORE DESIGNS

[Core diameter, 35.1 cm; maximum fuel-cladding temperature, 1805 K.]

Average coolant pressure, MN/m^2	Average coolant pressure, psia	Fuel volume fraction	Free-flow volume fraction	Reynolds number	Fuel-pin diameter, cm	Average fuel center-line temperature in hot channel, K	Maximum fuel center-line temperature, K
[a]1.72	248	0.525	0.152	1.93×10^4	1.54	2080	2310
2.76	400	.624	.092	2.97	2.54	2530	[b]2870

[a]Reference value from cycle study.
[b]Exceeds UO_2 melting point of 2750 K.

a 19-percent increase in fuel volume fraction (table VI). However, the increase in fuel-pin diameter caused the fuel centerline temperature to exceed 2750 K, the melting point of UO_2, thereby nullifying this configuration.

The significant increase in fuel temperature in table VI was indicative of calculations at other parametric conditions. Even at maximum fuel-cladding temperatures of 1770 K (the lowest temperature considered herein) fuel temperatures, although below the UO_2 melting point, were in the range of 100-percent release of fission gases. Consequently, with the assumptions given in table VI there appeared to be no advantage in increasing the coolant pressure.

Reactor Pressure Drop

Reactor pressure drop represents another parameter which was assigned a value from the cycle analysis. The potential in reactor design for core size reduction from a thermodynamics standpoint was investigated. Increasing the core pressure drop should reduce the required free-flow volume, thereby increasing the fuel volume fraction. As a result, core size would be reduced. The results for calculations on a core with reference-design parameter values and a maximum fuel-cladding temperature of 1805 K showed such an effect, although the magnitude was small (fig. 8).

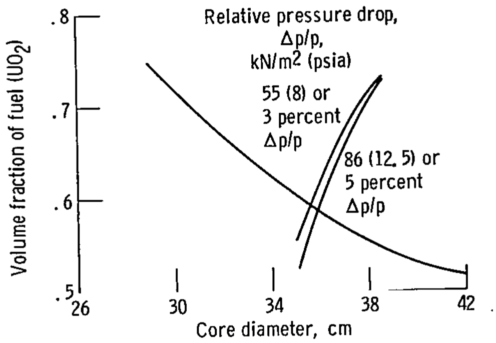

Figure 8. - Effect of pressure drop on size of pin core designs. Maximum fuel-cladding temperature, 1805 K; radial peak-to-average power ratio, 1.05.

TABLE VII. - EFFECT OF REACTOR PRESSURE DROP ON CHARACTERISTICS OF PIN CORE DESIGNS

[Core diameter, 35.1 cm; maximum fuel-cladding temperature, 1805 K.]

Relative pressure drop, percent	Reactor pressure drop[a]		Fuel volume fraction	Free-flow volume fraction	Fuel-pin diameter, cm	Reynolds number	Average fuel center-line temper-ature in hot channel, K	Maximum fuel center-line temper-ature, K
	kN/m^2	psia						
3	55	8	0.525	0.152	1.54	1.93×10^4	2080	2310
5	86	12.5	.560	.110	2.17	2.59	2360	2580

[a]Includes inlet and exit losses.

A more significant effect of increasing the pressure drop to 86 kilonewtons per square meter (12.5 psia), or an increase to 5-percent relative pressure drop, was the increase in fuel temperature (table VII). Consequently, even at a fuel-cladding temperature of 1770 K (the lowest temperature considered), fuel temperatures were in the assumed range of 100-percent fission gas release. As a result, fuel-cladding thickness increased, thereby reducing available fuel volume.

Fuel Material

Potential core size reduction by the use of a more dense fuel material was investigated by using uranium nitride ($U^{235}N$) in pin cores with the parameters listed in table I.

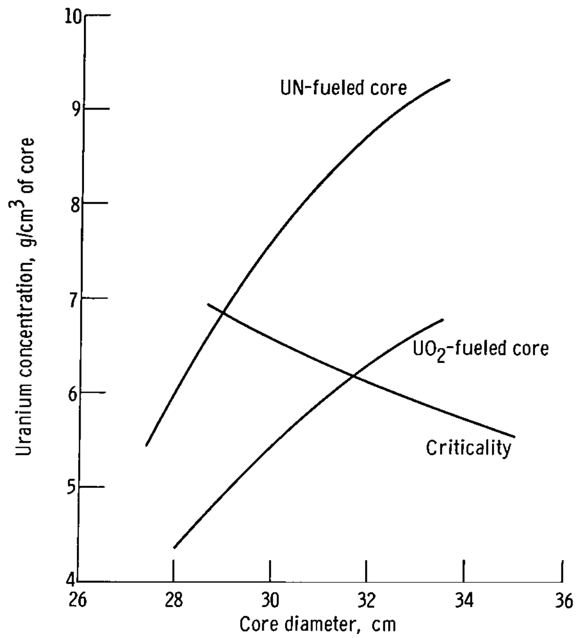

Figure 9. - Effect of fuel material on core size for pin cores. Maximum fuel-cladding temperature, 1805 K; radial peak-to-average power ratio, 1.05.

Because of the greater uranium density in UN the required core size was smaller for the same fuel volume fraction (compared with a UO_2 fueled core). Also, fuel temperatures were decreased due to the greater thermal conductivity of UN. A plot of the data in figure 9 indicates that the critical core diameter could be reduced by 8 percent if $U^{235}N$ were substituted for $U^{235}O_2$ in pin core designs.

In the above calculations, UN was assumed to behave identically to UO_2 with respect to fission gas release and material stability. Experimental data were considered to be too uncertain to warrant more specific design criteria.

SELECTED CORE DESIGN

Data generated in the neutronics and thermal-hydraulic analyses were used to determine a recommended set of design conditions. From these conditions the minimum core size that would satisfy the operational requirements was determined, and the resulting configuration was calculated. These results were summarized in table VIII. The reactor core was a right cylinder with a length-to-diameter ratio of 1. A pin core was selected over a matrix core because of its smaller size. Although structurally a number of problems are associated with pin cores (e.g., pin bowing and uneven flow distribution), the smaller size of the pin core was considered an overriding factor. Radial BeO reflectors, 7.62 centimeters thick, were shown to provide an adequate control range. No attempt was made to optimize reflector thickness. Similarly, 1.27-centimeter-thick tungsten

TABLE VIII. - SELECTED CORE DESIGN CHARACTERISTICS

General:	
Power, MW thermal	1
Core life, hr	25 000
Fuel type	Enriched $U^{235}O_2$ fuel pins
Coolant	He-60Xe
Control system	Axially moving radial reflectors
Neutronic:	
Cold-clean multiplication factors:	
Radial reflectors closed	1.05
Operating control reflectors open	1.04
All reflectors open	0.86
Leakage flux at 0.1 MeV, neutrons/cm^2	3×10^{13}
Peak-to-average power:	
Radial	1.05
Axial	1.31
Peak burnup, fission/cm^3 UO_2	1.54×10^{20}
Median fission energy, MeV	0.35
Thermal-hydraulics:	
Coolant temperature, K:	
Inlet	1190
Outlet	1650
Coolant pressure, MN/m^2; psia:	
Inlet	1.74 (252)
Outlet	1.68 (244)
Maximum fuel-cladding temperature, K	1805
Maximum fuel temperature, K	2210
Maximum heat flux, W/cm^2	19
Average heat-transfer coefficient, J/(cm^2)(K); Btu/(hr)(ft^2)(^{o}F)	1010 (178)
Configuration:	
Fuel:	
Material	$U^{235}O_2$
Length, cm	31.7
Diameter, cm	1.01
Fuel pins:	
Material	W-25Re
Number	662
Pitch, cm	1.18
Length, cm	34.87
Outside diameter, cm	1.12
Inside diameter, cm	1.04
Pressure vessel:	
Material	W-25Re
Inside diameter, cm	31.7
Wall thickness, cm	0.95
Radial reflectors:	
Material	BeO
Length, cm	31.7
Thickness, cm:	
Inner section	6.62
Outer section	1.0
End plates:	
Material	W
Diameter, cm	31.7
Thickness, cm	1.27

end plates were considered to be adequate. The fuel pins were W-25Re tubes loaded with enriched $U^{235}O_2$ and were arranged in a triangular lattice. The use of $U^{235}N$ fuel to reduce core size was rejected because of lack of material data.

Values for coolant inlet temperature, average coolant pressure, and reactor pressure drop were determined to be 1190 K, 1.72 meganewtons per square meter (248 psia), and 3 percent $\Delta P/P$ or 55 kilonewtons per square meter (8 psia), respectively, by cycle analyses, and no incentive was found in core size reduction to change these values. Maximum fuel-cladding temperature was set at 1805 K; higher values required excessive fuel cladding and lower values necessitated very small fuel pins. Radial power flattening was necessitated by excessive core temperatures. Although power ratios of 1.10 and 1.05 resulted in about the same core size, the use of 1.05 was preferred because of consequent lower fuel temperatures. No appreciable core size reduction was attained by increasing the fission gas containment volume from 10 to 20 percent of the core because at design conditions the fuel-cladding thickness was already near the 0.025-centimeter minimum.

SUMMARY OF RESULTS

A recommended design evolved from a study for the preliminary design of a gas-cooled reactor that would produce 1 megawatt of heat for 25 000 hours with a coolant outlet temperature of 1650 K. The principal restraints imposed on the design were (1) fission gases must be completely contained within the core, (2) creep in the fuel cladding could not exceed 1 percent over the core life, (3) a minimum of 10-percent reactivity control must be available from radial reflector movement, and (4) in the cold-clean, critical condition 5-percent excess reactivity control must be available. The resulting reactor design had the following characteristics:

1. The core was a right cylinder (length = diam = 31.7 cm) composed of pins fueled with $U^{235}O_2$, with a 10-percent void space for fission gases at the coolant inlet end, and cooled with He-60Xe flowing at 8.5 kilograms per second.

2. Reactivity control was achieved by axial movement of 7.62-centimeter beryllium oxide radial reflectors.

3. Design conditions were as follows: coolant inlet temperature, 1190 K; average core pressure, 1.71 meganewtons per square meter (248 psia); reactor pressure drop, 55 kilonewtons per square meter (8 psia or 3 percent $\Delta P/P$); power distribution, radial peak-to-average ratio of 1.05.

Results from parametric analyses performed in the reactor design study are as follows:

1. Exclusive of structural limitations, the size of pin cores decreases with decreasing fuel-cladding temperature. The effect on required core size of lower heat transfer per unit area at lower temperatures was offset by the effect of reduced fuel-cladding thickness.

2. In pin core designs the maximum fuel-cladding temperature was limited to the range of 1770 to 1840 K. At lower temperatures the fuel-pin diameter was reduced below the minimum allowable value of 0.5 centimeter, and at higher cladding temperatures the melting point of UO_2 was exceeded at the fuel centerline.

3. The minimum size for pin cores was attained with a maximum fuel-cladding temperature of 1805 K. At lower temperatures the assumed minimum thicknesses of 0.025 centimeter was reached. At higher temperatures, the effect of improved heat transfer per unit area was more than offset by the effect of increased cladding thickness.

4. The minimum size for matrix cores was attained at the maximum fuel temperature where fission gases were retained in the fuel material. This was assumed to be 1890 K at the fuel surface.

5. Radial power flattening in pin core designs to a peak-to-average power ratio of 1.1 resulted in a 9-percent reduction of core diameter. An additional 1-percent reduction was achieved by reducing the power ratio to 1.05.

6. Less than a 1-percent-diameter reduction of pin core designs resulted from increasing the size of the fission gas containment chamber from 10 to 20 percent of the core volume because fuel-cladding thicknesses were reduced to the assumed fabrication lower limit of 0.025 centimeter.

7. Core size was not sensitive to variations of the chopped cosine shape factor for axial power distribution. Variation of the ratio of extrapolated length to fueled length from 1.27 to 1.5 resulted in less than a 1-percent increase in core diameter.

8. Core diameter varied ±1 percent for variations of ±60 K in the coolant inlet temperature of pin core designs.

9. Increasing the coolant pressure from 1.72 to 2.76 meganewtons per square meter (248 to 400 psia) would have reduced core size except for the fact that the resulting fuel temperatures exceeded the melting point of UO_2, thereby violating a design procedure criterion.

10. Increasing the reactor pressure drop from 55 to 86 kilonewtons per square meter (8 to 12.5 psia) also would have reduced core size except for the fact that the increased fuel temperatures caused 100-percent release of fission gases. The resulting increased fuel-cladding thicknesses caused core size to increase.

11. The critical diameter of a matrix core was 37 percent larger than a pin core, primarily because of the lower uranium density in the matrix fuel material.

12. If the same fission gas release criteria were assumed, a potential reduction of

8 percent in core diameter would result from the use of $U^{235}N$ in place of $U^{235}O_2$ as the fuel material for pin core designs.

Lewis Research Center,
National Aeronautics and Space Administration
Cleveland, Ohio, October 31, 1968,
120-27-06-05-22.

APPENDIX A

SELECTION OF CYCLE CONDITIONS

In order to establish reactor design conditions it was first necessary to establish a conceptual power system and select a reference set of cycle parameters. Cycle performance variations were investigated to establish reactor inlet pressure, temperature, and working fluid molal flow rate. Then turbomachinery staging and sizing calculations were performed to determine working-fluid molecular weight and pressure level.

A temperature-entropy diagram of the power conversion system showing the cycle state points is presented in figure 10. A single gas-loop system with a dual-shaft turbomachinery arrangement is assumed. The working fluid is assumed to be a mixture of helium and xenon (ref. 9).

Thermodynamic Calculations

The thermodynamic analysis was performed by using the procedure and equations presented in references 10 and 11. The assumed values of the fixed cycle parameters are presented in table IX along with the range of selected variables (recuperator effectiveness E; cycle temperature ratio T_4/T_1; and compressor pressure ratio p_5/p_4).

A system loss pressure ratio (i.e., that portion of the compressor pressure ratio which is available to the turbine) of 0.90 is assumed to be the practical upper limit of an all-gas conversion system. For this value of loss pressure ratio the assumed reactor pressure drop $\Delta p/p$ is 0.03 with the remaining 0.07 allowance for the radiator, recuperator, and connecting piping.

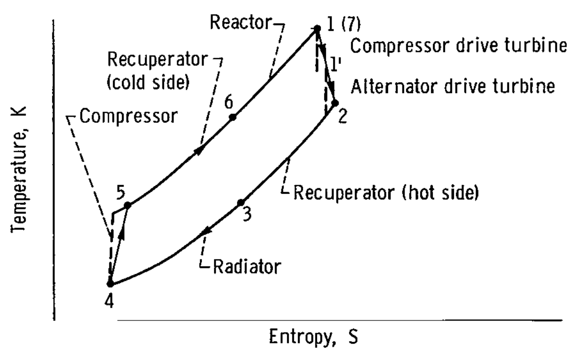

Figure 10. - Brayton-cycle temperature - entropy diagram.

TABLE IX. - ASSUMED CYCLE PARAMETERS AND RANGE OF

VARIABLES FOR THERMODYNAMIC CALCULATIONS

Parameter	Assumed value or range
Turbine inlet temperature, K	1650
Specific-heat ratio	1.667
Turbine efficiencies	0.88
Compressor efficiency	0.80
Loss pressure ratio	0.90
Radiator convective-heat-transfer coefficient, $W/(m^2)(K)$	140
Radiation sink temperature, K	220
Radiator emissivity	0.86
Recuperator effectiveness	0.60 to 0.90
Cycle temperature ratio	0.28 to 0.34
Compressor pressure ratio	1.8 to 3.0

Recuperator effectiveness. - It has previously been shown (refs. 12 and 13) that high values of effectiveness E are desirable for high cycle efficiency and low radiator area. A small temperature rise through the reactor is also desirable to reduce thermal stresses in the reactor core. The effect of recuperator effectiveness on working-fluid temperature rise through the reactor ΔT is presented in figure 11 for a range of compressor pressure ratios. The effect of E on ΔT is quite significant, especially at low values of compressor pressure ratio. An increase of 0.1 in E reduces ΔT by as much as 72 K.

Although a high value of effectiveness improves cycle performance and reduces ΔT, as E is increased the recuperator weight and volume also increase. The analysis necessary to determine the optimum compromise between recuperator volume and cycle performance is beyond the scope of this report. Therefore, a value of 0.80 was selected as representing a reasonable upper limit for recuperator effectiveness.

Cycle temperature ratio. - The effects of cycle temperature ratio on specific prime radiator area A_r/P_{sh} and cycle efficiency η_{cy} are presented in figure 12. The optimum cycle performance envelope is presented as the curve drawn tangent to the individual cycle temperature ratio curves. The figure shows that minimum area occurs at a cycle temperature ratio of 0.31, a compressor pressure ratio of 2.8, and an efficiency of 0.242.

At the selected effectiveness of 0.80, a 0.01 change in cycle temperature ratio changes ΔT by less than 6 K, as shown in figure 11. The cycle temperature ratio, although necessary to establish the cycle point, has only a minor effect on ΔT and,

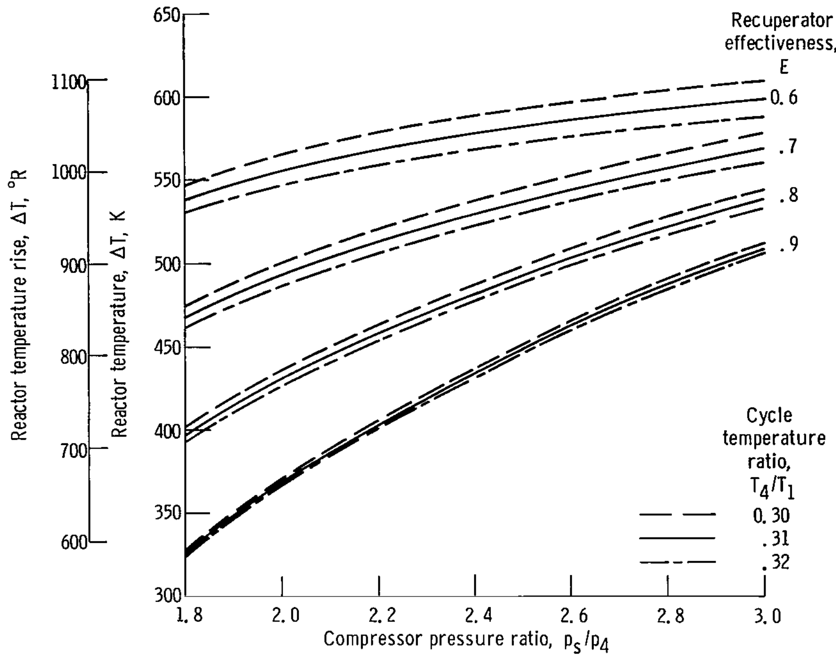

Figure 11. - Effect of compressor pressure ratio and recuperator effectiveness on reactor temperature rise with fuel-pin length of 0.90.

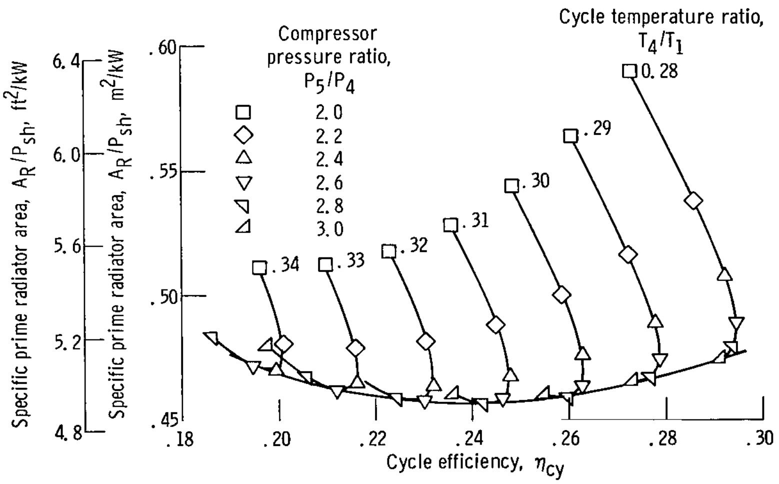

Figure 12. - Brayton-cycle characteristic curves at recuperator effectiveness of 0.80 and loss pressure ratio of 0.90.

therefore, has little effect on the reactor design itself.

For this high-power system, minimum system weight and volume are important, so that operation near the minimum area is desired (refs. 11 and 13). Therefore, a cycle temperature ratio of 0.31 was selected as the reference value.

Compressor pressure ratio. - The effects of compressor pressure ratio on radiator area and cycle efficiency are shown in figure 12. For the selected design conditions, minimum area occurs at a pressure ratio of 2.8. In order to reduce the expected high number of turbomachinery stages (ref. 14), it was considered desirable to accept a small area penalty by moving off the minimum of the temperature ratio curve and selecting a pressure ratio of 2.2. This reduction of pressure ratio increases A_R/P_{sh} by 7 percent, but also increases cycle efficiency slightly. A further reduction of pressure ratio is desirable because area increases at an ever increasing rate and efficiency is also significantly reduced. This reduction in pressure ratio to 2.2 also has a favorable effect on ΔT, reducing it from 520 to 460 K. An increase in cycle temperature ratio to reduce the area was not considered because a small savings in area requires a significant reduction in cycle efficiency.

With the selection of compressor pressure ratio, cycle temperature ratio, and recuperator effectiveness, the cycle is defined. The reactor parameters obtained from the cycle calculations are a specific capacity rate w_{Cp}/P_{sh} of 8.9×10^{-3} K^{-1}, a working-fluid inlet temperature T_6 of 1190 K, and a reactor pressure loss of 0.03.

Working-Fluid Selection

Because of the severe stress limitations imposed on the turbines by the high-temperature and long-life requirements, a large number of turbomachinery stages are required. While a high-molecular-weight working fluid is desired to reduce the required turbomachinery stages, consideration should be given to the increasing heat exchanger size with molecular weight. The use of a helium-xenon mixture, rather than a single gas with the same molecular weight, improves heat exchanger performance because of the improved heat-transfer properties (ref. 9). A working-fluid molecular weight of 80 with heat-transfer properties similar to those of argon but requiring only one-half the turbomachinery stages that argon requires was assumed.

At the selected molecular weight an estimate of the required turbine stages was obtained by the method outlined in reference 14, while the compressor stages were estimated by a specific-speed analysis (ref. 15). The following assumptions were made for the turbine analysis: (1) a hub- to tip-radius ratio of 0.818, (2) a constant mean diameter, (3) equal work per stage, (4) a stage-speed-work parameter of 1, (5) stress-limited blades, and (6) a first-stage rotor temperature 56 K below the turbine inlet temperature.

The compressor was assumed to have equal work per stage and a specific speed corresponding to maximum efficiency. The assumed turbine material is a tantalum alloy (NAS-39) which is presently under development (ref. 16). The stress data are based on 1/2 percent creep in 25 000 hours. Only axial-flow machines were considered because of the problems of staging radial machines. A rotational speed of 12 000 rpm (1260 rad/sec) was assumed for both shafts because of the turbine stress limitations. Also, this shaft speed is compatible with 400-hertz alternator output.

The results of the staging analysis show that, with a molecular weight of 80, the dual-shaft arrangement requires a five-stage high-pressure turbine, about 14 compressor stages, and a single-stage low-pressure turbine. Although a rather large number of turbomachinery stages are required, a reduction of several stages can be realized by allowing the latter stages, where the temperature is lower, to operate at higher tip speeds and perform more work than the initial stages (ref. 14). The working-fluid mass flow rate is determined from the specific capacity rate, the heat capacity of the fluid, and the product of cycle efficiency and reactor thermal power. With a molecular weight of 80 and a reactor thermal power of 1 megawatt, the working-fluid mass flow rate is 8.5 kilograms per second.

Working-fluid pressure level. - The remaining system parameter, working-fluid pressure at the reactor inlet, needed for the reactor design is determined by a procedure outlined in reference 14 and based on the low-pressure-turbine diameter. At the rotational speed of 12 000 rpm (1260 rad/sec), a hub- to tip-radius ratio of 0.818, and limiting tip speed, the low-pressure-turbine diameter is 35.6 centimeters. At this diameter the low-pressure-turbine outlet pressure p_2 is 0.88 meganewton per square meter (128 psia). At the design condition ($p_5/p_4 = 2.2$; $L = 0.90$) the high-pressure-turbine inlet pressure p_1 is 1.68 meganewtons per square meter (244 psia) and its diameter is 20 centimeters. Based on the assigned reactor pressure drop of 0.03, the reactor inlet pressure is 1.74 meganewtons per square meter (252 psia).

APPENDIX B

PRESSURE VESSEL THICKNESS

One percent creep over the core lifetime was selected as the design criterion. Based on a design temperature of 1650 K, an allowable design stress σ_f of 49 meganewtons per square meter (7100 psia) was obtained from a Larson-Miller correlation for 1-percent creep over 25 000 hours in W-25Re (fig. 13). Application of a safety factor of 1.25 reduced the design stress to 39 meganewtons per square meter (5700 psia). The minimum wall thickness for thin-walled cylinders is then

$$t = \frac{pD}{2} \tag{1}$$

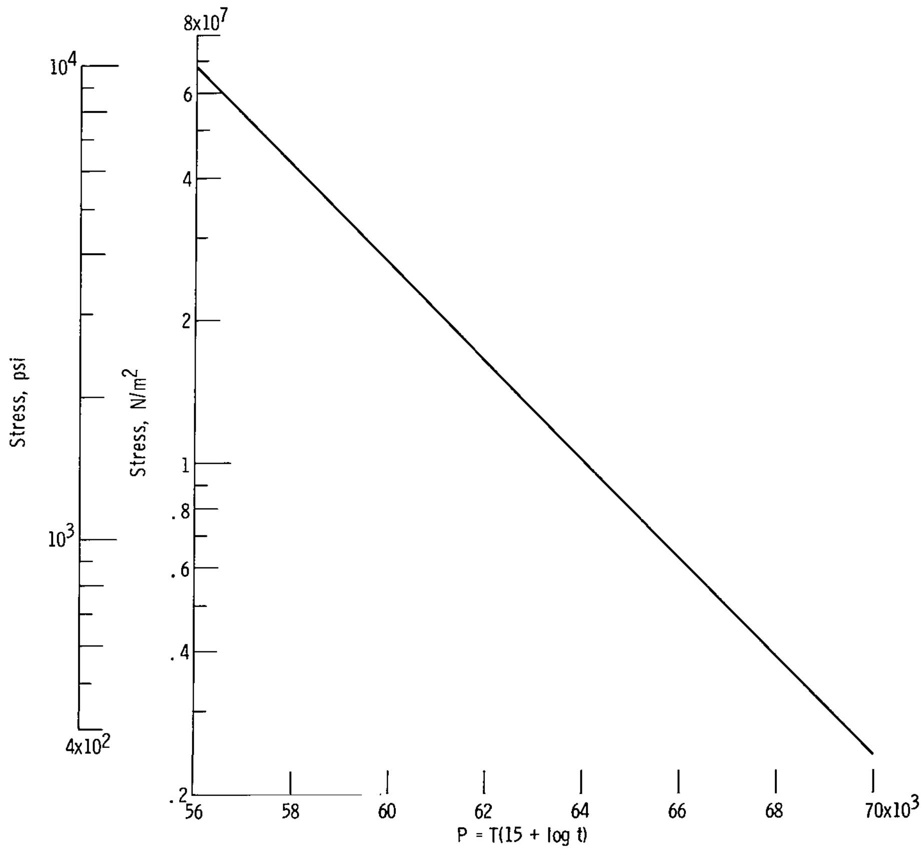

Figure 13. - Larson-Miller correlation of experimental data for 1-percent creep in tungsten - 25-weight-percent rhenium (where P is in °R, and t is time in hours).

where p is the coolant gas pressure, and D is the core diameter.

$$t = \frac{250\ D}{2(5700)} = 0.0219\ D$$

For a core diameter range of 30 to 44 centimeters, the wall thickness is 0.66 to 0.97 centimeter. Since a wall thickness variation of this magnitude was shown to be unimportant to the neutronics analysis (ref. 4), a constant value of 0.95 centimeter (3/8 in.) was selected for all core sizes in the study.

The W-25Re alloy was substituted for tungsten (which was used in the neutronics analysis) because of its better fabricability. Any effect on calculated reactivities was considered to be insignificant.

APPENDIX C

REFLECTOR HEATING

Heating calculations were performed to determine the necessity for forced cooling of the reflector. A one-dimensional heat-transfer model was utilized which considered radiation and convection from the core to the pressure vessel, and radiation between the pressure vessel, reflector, and heat sink to be the dominant processes. Additional heating occurred from interactions with neutrons and gamma rays.

The use of 0.5 for the emissivities of all radiating surfaces was considered to be a reasonably realistic approach in view of the lack of high-temperature data. For the

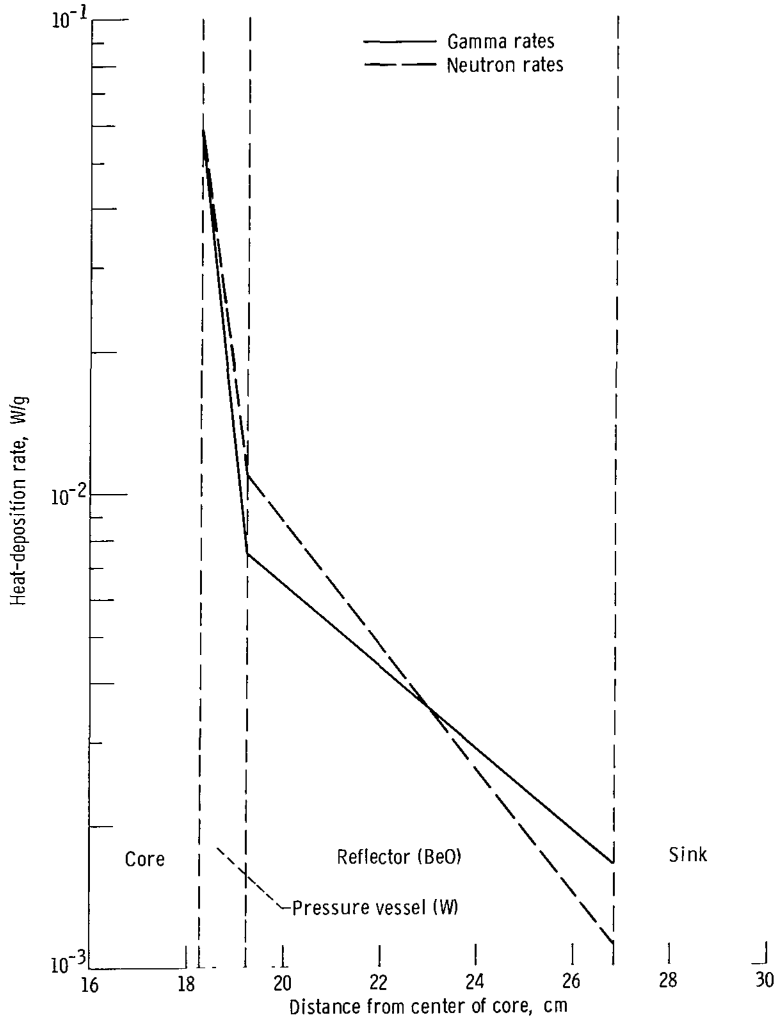

Figure 14. - Gamma and neutron mass heating rates in reflector and pressure vessel.

limiting case all surfaces were considered to be black. The heat sink was considered to be black for all cases, and its temperature was varied from K (approximating deep space) to 1000 K (simulating a shield). The reactor model was a 33.5-centimeter-diameter core surrounded by a 0.95-centimeter-thick tungsten pressure vessel and a 7.62-centimeter-thick BeO radial reflector. A 0.62-centimeter gap separated the pressure vessel and the reflector. Both BeO and niobium (Nb) were used as reflector materials to indicate the effect of thermal conductivity.

Heat-deposition rates from gamma rays were calculated with the QAD code (ref. 17), whereas neutron heat-deposition rates were estimated from flux distributions obtained from criticality calculations. Both heating rates exhibited an exponential decrease with increasing distance through the pressure vessel and the reflector regions (fig. 14). Calculations were made along the radial centerline to obtain maximum values. However, the nuclear heating contribution to reflector temperatures was later shown to be less than 2 percent of the total.

Results from the reflector heating calculations, summarized in table X, indicate a maximum reflector temperature of about 1500 K, which occurs at the inside surface. This would seem to be within the capability of the material, and, therefore, forced cooling should not be necessary. A maximum temperature gradient of about 50 K per centimeter occurred in the reflector. The significance of this gradient could not be determined without a mechanical design.

TABLE X. - RESULTS OF REFLECTOR TEMPERATURE ANALYSIS

Core axial location	Reflector material	Emissivity	Heat sink	Pressure vessel	Reflector inside surface	Reflector outside surface
			Temperature, K			
Center	BeO	1.0	0	1455	1316	1010
	BeO	.5	0	1433	1185	1025
	BeO	.5	500	1435	1194	1036
	BeO	.5	800	1442	1230	1092
	Niobium	.5	0	1422	1112	1056
Exit	BeO	1.0	0	1620	1484	1095
	BeO	.5	0	1584	1314	1110
	BeO	.5	1000	1604	1406	1223
	Niobium	.5	0	1569	1229	1146

APPENDIX D

COOLANT INLET AND OUTLET PRESSURE LOSSES

Pressure losses due to contraction of the coolant at the core inlet and expansion of the coolant at the core outlet can be expressed as multiples of velocity heads (ref. 18) as follows:

Contraction loss:

$$\Delta p_i = K_c \frac{\rho_i v_i^2}{2g} \tag{2}$$

Expansion loss:

$$\Delta p_o = K_e \frac{\rho_o v_o^2}{2g} \tag{3}$$

where

ρ coolant density

v coolant velocity

K_c contraction coefficient

K_e expansion coefficient

g gravitational acceleration

and the subscripts i and o indicate inlet and outlet conditions, respectively.

For a representative pin core design with the parameters from table I, a diameter of 31.7 centimeters, and a free-flow volume fraction of 0.186, the calculated inlet and outlet coolant velocities were 40 and 57 meters per second, respectively. The coefficients K_c and K_e were evaluated from figures 1.6 and 1.5 of reference 18 to be 0.38 and 0.65, respectively. The pressure losses were then

$$\Delta p_i = \frac{(0.38)(14.1\ \mathrm{kg/m^3})(40\ \mathrm{m/sec})^2}{(2)(9.8\ \mathrm{m/sec^2})} = 437\ \mathrm{kg/m^2} = 4280\ \mathrm{N/m^2}$$

$$\Delta p_o = \frac{(0.65)(9.95\ \mathrm{kg/m^3})(57\ \mathrm{m/sec})^2}{(2)(9.8\ \mathrm{m/sec^2})} = 1070\ \mathrm{kg/m^2} = 10\ 500\ \mathrm{N/m^2}$$

$$\Delta p_T = 55\ \mathrm{kN/m^2}$$

$$\frac{\Delta p_i + \Delta p_o}{\Delta p_T} = \frac{0.00428 + 0.0105}{0.055} = 0.27 = 27\ \text{percent}$$

APPENDIX E

COMPRESSIBLE FLOW AS COMPARED TO INCOMPRESSIBLE FLOW

To simplify calculations in this study incompressible flow equations were used to describe the behavior of the coolant gas. The accuracy of this procedure was checked as follows:

For compressible flow through a heated channel (from ref. 19)

$$\frac{dp_o}{p_o} = \frac{-\gamma M^2}{2}\left(\frac{dT_o}{T_o} + f\frac{dZ}{D_e}\right) \tag{4}$$

where

p_o pressure at stagnation condition

γ ratio of specific heats at constant pressure and volume

M Mach number

T_o absolute temperature at stagnation condition

f Darcy-Weisbach friction factor

Z direction along length of channel

D_e hydraulic diameter of channel

For small M, $dp_o/p_o = dp/p$ and $dT_o/T_o = dT/T$, and, therefore, integration over the length of the reactor yields

$$\ln\frac{p_2}{p_1} = \frac{-\gamma\overline{M}^2}{2}\left(\ln\frac{T_2}{T_1} + \frac{\bar{f}L_p}{D_e}\right) \tag{5}$$

where subscripts 1 and 2 refer to inlet and outlet conditions, respectively, and $\overline{M}$ and $\bar{f}$ are values averaged over the core length.

For small values of the right side of equation (5)

$$\frac{p_2}{p_1} = 1 - \frac{\gamma\overline{M}^2}{2}\left(\ln\frac{T_2}{T_1} + \frac{\bar{f}L_p}{D_e}\right)$$

and the core pressure drop for compressible flow (excluding inlet and exit effects) is

$$\Delta p_c = p_1 - p_2 = \frac{\gamma \overline{M}^2 p_1}{2}\left(\ln \frac{T_2}{T_1} + \frac{\bar{f} L_p}{D_e}\right) \tag{6}$$

The core pressure drop for incompressible flow is (ref. 7)

$$\Delta p_{inc} = \frac{\bar{f} L_p}{D_e} \frac{\bar{\rho} \overline{V}^2}{2 g_c} \tag{7}$$

where

$\bar{\rho}$ average coolant density

$\overline{V}$ average coolant velocity

g_c acceleration due to gravity

Substituting equation (7) into equation (6) and using the definition of Mach number,

$$\overline{M} = \frac{\overline{V}}{g_c \gamma \left(\frac{\bar{p}}{\bar{\rho}}\right)^{1/2}}$$

yields

$$\frac{\Delta p_c}{\Delta p_{inc}} = \frac{p_1}{\bar{p}}\left(\frac{D_e}{\bar{f} L_p} \ln \frac{T_2}{T_1} + 1\right) \tag{8}$$

To illustrate the magnitude of these pressure drops a representative core design was chosen with the following conditions:

(1) Fuel length equal to core diameter, 33.5 centimeters
(2) Ratio of pin length to fuel length L_p/L, 1.1
(3) Inlet pressure p_1, 1.74 meganewtons per square meter (252 psia)
(4) Average pressure $\bar{p}$, 1.72 meganewtons per square meter (248 psia)
(5) Hydraulic diameter of channel D_e, 0.244 centimeter
(6) Peak-to-average radial power ratio $(P_p/\overline{P}_R)$, 1.05
(7) Average Darcy-Weisbach friction factor $\bar{f}$, 0.024

(8) Outlet temperature T_2, 1650 K

(9) Inlet temperature T_1, 1190 K

Substitution into equation (8) yields

$$\frac{\Delta p_c}{\Delta p_{inc}} = 1.10$$

that is, the calculated core pressure drop from compressible flow equations is 10 percent greater than that calculated by the incompressible flow equations.

APPENDIX F

FUEL-CLADDING STRESS LIMIT

On the premise that the creep rate of a material is independent of prior creep sustained at other conditions, an analytical method was developed relating creep at constant stress to creep in a linearly increasing stress environment (ref. 20). If the Larson-Miller method is used for correlating creep data, the stress-deformation relation takes the form

$$\sigma_f = \frac{\epsilon_o}{\epsilon_f} \sigma_{LM} \left(1 - \frac{1}{mT}\right)^{-mT} \tag{9}$$

where

σ_f end-of-core-life stress in material

ϵ_o deformation basis of Larson-Miller plot of experimental data

ϵ_f allowable creep (deformation) at end of core life

σ_{LM} allowable stress from Larson-Miller plot based on constant stress over core life

m slope of Larson-Miller plot

T absolute temperature of material

Utilizing data from the Larson-Miller correlation (fig. 13) and equation (9) resulted in a curve relating allowable stress in the fuel cladding at the end of core life to the cladding temperature (fig. 15). Thus, for the core conditions of a 25 000-hour life, constant temperature, and constant rate of fission gas production (linearly increasing pressure and consequently stress), allowable stress can be read directly from figure 15.

A series of design calculations were made to show what effect the method used to calculate allowable creep stress in the wall of the fuel pin would have on required core size. Variable stress calculations utilized equation (9) (fig. 15) to determine the allowable stress to attain 1-percent creep in 25 000 hours, whereas constant-stress calculations were based on a constant stress (evaluated at the maximum fission gas pressure) existing over the entire core life. Core designs were evaluated at reference parameter values (table I) and a maximum fuel-cladding temperature of 1805 K. The results plotted in figure 16 indicated that a 3-percent decrease of critical core diameter was attained by using the variable stress calculational method. However, the magnitude of this effect was sensitive to core composition, which in turn was determined by design conditions. To

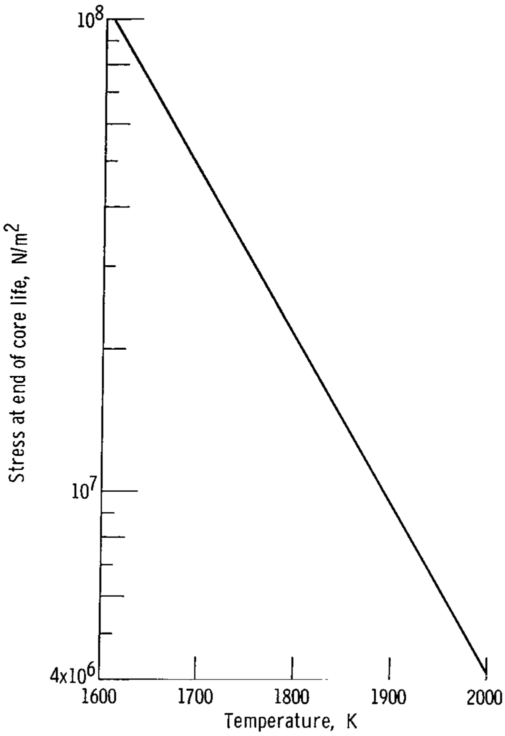

Figure 15. - Allowable end-of-life stress for 1-percent creep of tungsten - 25-weight-percent rhenium in linearly increasing stress environment. Core life, 25 000 hours.

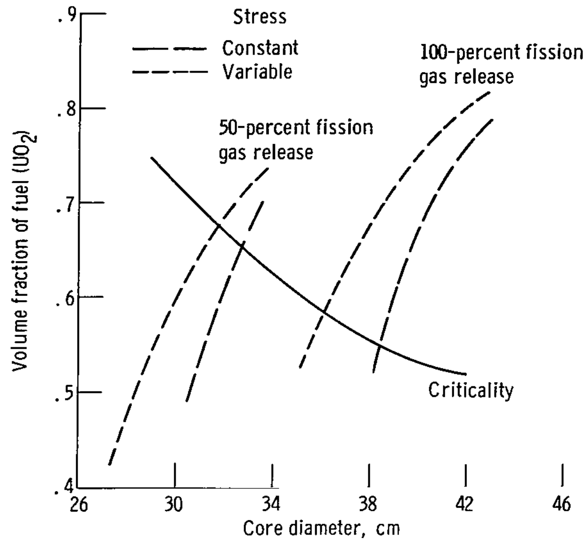

Figure 16. - Effect of creep calculational method on critical diameter of pin core designs. Maximum fuel-cladding temperature, 1805 K; radial peak-to-average power ratio, 1.05.

illustrate this, the calculations were repeated with the assumption of 100-percent fission gas release from the fuel. The increased quantity of fuel cladding in the core emphasized the effect of the variable stress calculational method and therefore a 6-percent reduction of critical core diameter was obtained.

APPENDIX G

STRESS FROM FISSION GAS PRESSURE

If it is assumed that the fission gas production rate is constant during core operation, the resulting pressure in a confined space can be calculated by

$$P_{fg} = c \frac{V'_F}{V'_{fg}} N E_F f_{fg} B \overline{T}_{fg} \tag{10}$$

where

c	fuel constant, $N/(m^2)(K)$, 3.41 for UO_2 and 476 for UN
V'_F	specific fuel volume, cm/g of U^{235}
V'_{fg}	specific fission gas volume, cm^3/g of U^{235}
N	inert gas atoms generated per fission
E_F	uranium enrichment in the 235 isotope (U^{235}), percent
f_{fg}	fraction of fission gases released from fuel
B	fraction of fuel that fissions (burnup)
$\overline{T}_{fg}$	average absolute temperature of fission gases, K

Also included in equation (10) are the assumptions that the perfect-gas law is valid and that all fissions occur in U^{235}. The value of N was estimated to be 0.25 atom per fission (ref. 21).

For the fuel-pin geometry in figure 17 the volume of fuel available for fission gases was calculated from

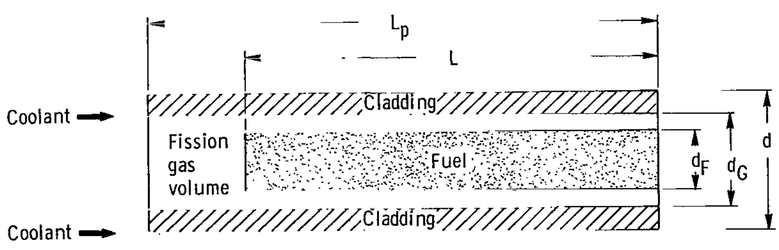

Figure 17. - Fuel-pin geometry.

V_{fg} = (Hot gap around fuel rod) + (Gas chamber at end of rod) + (Voids in fuel)

$$V_{fg} = \frac{\pi}{4}\left(d_G^2 L_p - f_p d_F^2 L\right) \tag{11}$$

where

d_G outside diameter of gap between fuel and cladding

L_p pin length

f_p ratio of actual fuel density to theoretical density

d_F outside diameter of fuel

L fuel length

and

$$\frac{V'_{fg}}{V'_F} \equiv \frac{V_{fg}}{V_F} = \left(\frac{d_G}{d_F}\right)^2 \frac{L_p}{L} - f_p \tag{12}$$

where the fuel volume $V_F \equiv \pi\left(d_F^2/4\right)L$. In order to allow for thermal expansion when the core temperature is brought to power, all these dimensions were evaluated at operating temperatures. A nominal temperature change of 1700 K was used to determine all dimensional changes.

The temperature of the fission gases varies both radially and axially. To select a single value to use in equation (10) the temperature in the gap was averaged over the core (both radially and axially). The resulting expression was

$$\overline{T}_{fg} = \left(\frac{P_p}{\overline{P}}\right)_R F_H \overline{T}_s + \left[1 - \left(\frac{P_p}{\overline{P}}\right)_R F_H\right] T_{f,i} + \frac{0.89 F_H dRe}{Lk_G} \left(\frac{P_p}{\overline{P}}\right)_R \ln \frac{d_G}{d_F} \tag{13}$$

where

$\left(\frac{P_p}{\overline{P}}\right)_R$ peak-to-average radial power ratio

F_H hot-channel factor

T_s axially averaged fuel-cladding temperature in an average channel

$T_{f,i}$	coolant inlet temperature
d	outside diameter of fuel cladding (pin)
L	fuel length
Re	Reynolds number
d_G	outside diameter of gap between fuel and cladding
d_F	diameter of fuel
k_G	equivalent conductivity across gap (ref. 18)

REFERENCES

1. Stewart, Warner L.; Anderson, William J.; Bernatowicz, Daniel T.; Guentert, Donald C.; Packe, Donald R.; and Rohlik, Harold E.: Brayton Cycle Technology. Space Power Systems Advanced Technology Conference. NASA SP-131, 1966, pp. 95-145.

2. Lubarsky, Bernard; and Shure, Lloyd I.: Applications of Power Systems to Specific Missions. Space Power Systems Advanced Technology Conference. NASA SP-131, 1966, pp. 269-285.

3. Freedman, S. I.; Keiser, J. T.; Cohen, R. M.; and Terrill, W. R.: Nuclear Brayton Cycle Powerplants for Space Applications. Advances in Energy Conversion Engineering. ASME, 1967, pp. 749-769.

4. Whitmarsh, Charles L., Jr.; and Kerwin, Paul T.: A 1-Megawatt Reactor Design for Brayton-Cycle Space Power Application. II - Neutronics Design. NASA TN D-5014, 1968.

5. Whitmarsh, C. L., Jr.: Reactivity Effects Caused by Radial Power Flattening in a Small, Fast-Spectrum Reactor. NASA TN D-4459, 1968.

6. Hardy, H. K.; Wyatt, L. M.; and Pugh, S. F.: Metallurgy of Fuel and Cans. J. Brit. Nucl. Energy Soc., vol. 2, no. 2, Apr. 1963, pp. 236-245.

7. El-Wakil, Mohamed M.: Nuclear Power Engineering. McGraw-Hill Book Co., Inc., 1962, p. 243.

8. Humble, Leroy V.; Lowdermilk, Warren H.; and Desmon, Leland G.: Measurements of Average Heat-Transfer and Friction Coefficients for Subsonic Flow of Air in Smooth Tubes at High Surface and Fluid Temperatures. NACA Rep. 1020, 1951.

9. Vanco, Michael R.: Analytical Comparison of Relative Heat-Transfer Coefficients and Pressure Drops of Inert Gases and Their Binary Mixtures. NASA TN D-2677, 1965.

10. Glassman, Arthur J.; and Stewart, Warner L.: Thermodynamic Characteristics of Brayton Cycles for Space Power. J. Spacecraft Rockets, vol. 1, no. 1, Jan.-Feb. 1964, pp. 25-31.

11. Glassman, Arthur J.: Thermodynamic and Turbomachinery Concepts for Radioisotope and Reactor Brayton-Cycle Space Power Systems. NASA TN D-2968, 1965.

12. Klann, John L.: Analysis and Selection of Design Conditions for a Radioisotope Brayton-Cycle Space Powerplant. NASA TN D-4600, 1968.

13. Glassman, Arthur J.: Summary of Brayton Cycle Analytical Studies for Space-Power System Applications. NASA TN D-2487, 1964.

14. Kofskey, Milton G.; and Glassman, Arthur J.: Turbomachinery Characteristics of Brayton Cycle Space-Power Generation Systems. Presented at the ASME 9th Annual Gas Turbine Conference and Products Show, Houston, Mar. 1-5, 1964.

15. Shepherd, D. G.: Principles of Turbomachinery. The MacMillan Co., 1956.

16. Moss, Thomas A.: Materials Technology Presently Available for Advanced Rankine Systems. Nucl. Appl., vol. 3, no. 2, Feb. 1967, pp. 71-81.

17. Malenfant, Richard E.: QAD: A Series of Point-Kernel General-Purpose Shielding Programs. Rep. LA-3573, Los Alamos Scientific Lab., Apr. 5, 1967.

18. McLain, Stuart; and Martens, John H., eds.: Engineering. Vol. 4 of Reactor Handbook. Second ed., Interscience Publ., 1964, pp. 207-208.

19. Shapiro, Ascher H.: The Dynamics and Thermodynamics of Compressible Fluid Flow. Vol. I. Ronald Press Co., 1953.

20. Whitmarsh, Charles L., Jr.: Method for Calculating Allowable Creep Stress in Linearly Increasing Stress Environment. NASA TN D-4352, 1968.

21. Etherington, Harold, ed.: Nuclear Engineering Handbook. McGraw-Hill Book Co., Inc., 1958, pp. 11-12 to 11-24.

NASA-Langley, 1969 —— 22 E-4665

"The aeronautical and space activities of the United States shall be conducted so as to contribute . . . to the expansion of human knowledge of phenomena in the atmosphere and space. The Administration shall provide for the widest practicable and appropriate dissemination of information concerning its activities and the results thereof."

— NATIONAL AERONAUTICS AND SPACE ACT OF 1958

NASA SCIENTIFIC AND TECHNICAL PUBLICATIONS

TECHNICAL REPORTS: Scientific and technical information considered important, complete, and a lasting contribution to existing knowledge.

TECHNICAL NOTES: Information less broad in scope but nevertheless of importance as a contribution to existing knowledge.

TECHNICAL MEMORANDUMS: Information receiving limited distribution because of preliminary data, security classification, or other reasons.

CONTRACTOR REPORTS: Scientific and technical information generated under a NASA contract or grant and considered an important contribution to existing knowledge.

TECHNICAL TRANSLATIONS: Information published in a foreign language considered to merit NASA distribution in English.

SPECIAL PUBLICATIONS: Information derived from or of value to NASA activities. Publications include conference proceedings, monographs, data compilations, handbooks, sourcebooks, and special bibliographies.

TECHNOLOGY UTILIZATION PUBLICATIONS: Information on technology used by NASA that may be of particular interest in commercial and other non-aerospace applications. Publications include Tech Briefs, Technology Utilization Reports and Notes, and Technology Surveys.

Details on the availability of these publications may be obtained from:

SCIENTIFIC AND TECHNICAL INFORMATION DIVISION

NATIONAL AERONAUTICS AND SPACE ADMINISTRATION

Washington, D.C. 20546